Numerical Study of Forced Convection in Wavy and Diverged-Converged Ducts

Dr. Waheed S. Mohamad*,Dr. Sattar J. Habeeb*& Mr. Anmar M. Basheer*

Received on: 28/9/2008
Accepted on:26/1/2009

Abstract

A three-dimensional study of developing fluid flow and heat transfer through wavy and diverged-converged ducts were studied numerically for a Prandlt number 0.7 and 5.85 and compared with flow through corresponding straight duct. The Navier-Stokes and energy equations are solved by using control finite volume method. Development of the Nusselt number in wavy and diverged-converged ducts are presented for different flow rates (50<Re<300), height ratio (H_{min}/H_{max}= 0.46, 0.39 and 0.33) for diverged-converged duct and length ratio (L/2a = 10, 6.67 and 5) for wavy duct. In the two types of ducts, the local Nusselt number increases with increasing of Reynolds number but decreases with decreasing height ratio or length ratio. In the diverged-converged duct at Pr=0.7 the maximum average Nusselt number takes place at height ratio (H_{min}/H_{max}=1) but it becomes minimum at Pr=5.85. The results shown that the best of heat transfer takes place at wavy duct compared to the diverged-converged duct when air heat exchanger is used. The water heat exchanger performance was found to be approximately similar for both ducts. There is good agreement between the results of this work with the corresponding numerical results presented by Bahaidarah et.al [9].

Keywords: forced convection, numerical study, wavy duct, diverged-converged duct

دراسة عددية للحمل القسري في مجرى متموج ومجرى متغير المقطع

الخلاصة

دراسة ثلاثية الابعاد لجريان مستقر وانتقال الحرارة لمائع خلال مجرى متموج واخر متغير المقطع لعدد برانتل 0.7 و 5.85 ومقارنة الجريان مع مجرى منتظم. حلت معادلة الطاقة والزخم بواسطة استعمال طريقة الفروقات العددية المحددة. ان عدد نسلت في المجرى المتموج والمتغير المقطع لمدى مختلف من التدفق (50<Re<300) , ونسبة الارتفاع (H_{min}/H_{max}) تساوي (0.46,0.39 and 0.33) للمجرى متغير المقطع. ونسبة الطول (L/2a) يساوي (10,6.67 and 5) للمجرى المتموج. ان عدد نسلت الموقعي لكلا النوعين يزداد بزيادة عدد رينولدز ولكن يقل بنقصان نسبة الطول. عند المجرى متغير المقطع يكون عدد نسلت الاجمالي للهواء اعلى مايمكن عندما تكون (H_{min}/H_{max}=1) (ولكنها تصبح ادنى مايمكن في حالة الماء. اظهرت النتائج بان افضل تبادل حراري يحدث للمجرى المتموج مقارنة بالمجرى متغير المقطع في حالة استخدام المبادل الحراري من نوع الهواء. اما البادل الحراري من نوع الماء فوجد ان الاداء يكون متشابة تقريبا لكلا المجريان. هناك توافق جيد بين النتائج التي تم الحصول عليها مع نتائج Bahaidarah et.al [9] .

NOMENCLATURE

a	Amplitude	m	T	Temperature	^{0}C
H	Height	m	U,V,W	Mean velocity components	m/s
L	Wavy length	m	W	width	m
Nu	Nusselt number		x,y,z	Cartesian coordinates	m
p	Pressure	N/m^2			
Pr	Prandlt number				
Re	Reynolds number				

* Mechanical Engineering Department, University of Technology / Baghdad

https://doi.org/10.30684/etj.27.7.14
2412-0758/University of Technology-Iraq, Baghdad, Iraq

Greek symbols

ρ	Density	kg/m^3
μ	Dynamic viscosity	kg/m.s
Ø	Dependent variable	
Γ	diffusion coefficient	
x,h,z	computational coordinates	m

Subscripts

min	Minimum
max	Maximum
in	Inlet condition
w	Condition at the wall

Introduction

An effective design for a heat exchanger is the one which maximized the heat transfer while reducing the power expended. Increase in surface area, which is the primary feature of many compact heat exchangers, invariably increases the heat transfer. However, this also increases the power expended and cost. There are several books and papers published on the basic design procedures of heat exchangers based on experimental and theoretical study of the past. However, some challenges of heat exchanger design will remain for fore-seeable future. This is due to the fact that the heat exchanger designs need to adopt itself to the ever growing process, power and aerospace industries. As these industries grow, more precise design of heat exchangers and suitable materials become crucial. The reduction in space occupied, better performance and cost effective design would be future objectives of the heat exchanger industry. **Hwang et.al, 2006[1]** investigated the flow and heat/mass transfer characteristics of wavy duct for the primary surface heat exchanger application. Local heat/mass transfer coefficients on the corrugated duct side walls are measured using a naphthalene sublimation technique. **Takachiro and Haruo, 2002[2]** applied the spectral element and finite difference methods using numerical studies on the three-dimensional laminar forced convection heat transfer in a channel with span wise-periodic fluted parts. **Blomerius et.al, 2000[3]** investigated flow field and heat transfer in sine-wave crossed-corrugated ducts by numerical solution of the Navier-Stokes and energy equations in the laminar and transitional flow regime between Re=170 and 2000. **Stone and Vanka, 1999[4]** presented numerical results on developing flow and heat transfer characteristics in a furrowed wavy channel The flow was assumed to be two-dimensional, and the Navier-Stokes equations governing a time-dependent flow were numerically solved. **Mamum et al, 2007[5]** investigated a natural-convection boundary layer along a vertical complex wavy surface with uniform heat flux. The complex surface study combines two sinusoidal functions, a fundamental wave and its first harmonic**. Mohamed et.al, 2006[6**] determined laminar forced convection in the entrance zone in a two dimensional converging-diverging channel with sinusoidal wall corrugation by using numerical simulation. The wavy surface of the channel lower wall is maintained to a temperature which is twice the upper wall temperature. Numerical solutions are obtained using the control-volume finite-difference method. **Manglik et.al, 2005[7]** presented detailed understanding forced convection in periodically developed low Reynolds number ($10 \leq Re \leq 1000$) air ($Pr = 0.7$) flows in three-dimensional wavy-plate-fin cores. Constant property computational solutions are obtained using finite-volume techniques for a non-orthogonal non-staggered grid. **Hossian and Sadrul Islam, 2007[8]** investigated fluid flow and heat transfer characteristics in wavy channels by using numerical solution of the Navier-Stokes and energy equations. Three different types of two dimensional wavy geometries (e. g. sine-shaped, triangular, and arc-shaped) are considered **Bahaidarah et.al, 2005[9]** presented detailed numerical steady two dimension fluid flow and heat transfer through a periodic wavy passage with a Prandlt number 0.7 and compared to flow through a corresponding straight (parallel-plate) channel. Sinusoidal and arc-shaped configurations were studied for a range of geometric parameters. At low Reynolds number, the two geometric configurations showed little or no heat transfer

augmentation in comparison with a parallel-plate channel. **Gradeck et.al, 2005[10]** performed study effects of hydrodynamic conditions on the enhancement of heat transfer for single phase flow. These experiments have been conducted for a wide range of Reynolds numbers, (0 < Re < 7500) in order to obtain the different regimes from steady laminar to turbulent.

The purpose of the present study is to test the prediction of three dimensional body fitted coordinate computational program which can be used to examine the effects of geometric parameters on the developed three dimensional fluid flow and heat transfer characteristics in wavy and diverged-converged ducts by using finite volume method.

Mathematical Model

The considered wavy and diverged-converged ducts are schematized in figure 1. The fluid flow is considered Newtonian, laminar, incompressible, and steady. Temperature value of the flow at inlet is double of the wall duct.

The fundamental equations describing the flow fields to be considered in three dimensional form of continuity, momentum (Navier-Stokes) and energy equations are [11]:

$$r\left(\frac{\partial U}{\partial x}+\frac{\partial V}{\partial y}+\frac{\partial W}{\partial z}\right)=0 \qquad (1)$$

$$r.\left[U\frac{\partial U}{\partial x}+V\frac{\partial U}{\partial y}+W\frac{\partial U}{\partial z}\right]= -\frac{\partial p}{\partial x}+m.\left(\frac{\partial^2 U}{\partial x^2}+\frac{\partial^2 U}{\partial y^2}+\frac{\partial^2 U}{\partial z^2}\right) \qquad (2a)$$

$$r.\left[U\frac{\partial V}{\partial x}+V\frac{\partial V}{\partial y}+W\frac{\partial V}{\partial z}\right]= -\frac{\partial p}{\partial y}+m.\left(\frac{\partial^2 V}{\partial x^2}+\frac{\partial^2 V}{\partial y^2}+\frac{\partial^2 V}{\partial z^2}\right) \qquad (2b)$$

$$r.\left[U\frac{\partial W}{\partial x}+V\frac{\partial W}{\partial y}+W\frac{\partial W}{\partial z}\right]= -\frac{\partial p}{\partial z}+m.\left(\frac{\partial^2 W}{\partial x^2}+\frac{\partial^2 W}{\partial y^2}+\frac{\partial^2 W}{\partial z^2}\right) \qquad (2c)$$

$$r\left(U\frac{\partial T}{\partial x}+V\frac{\partial T}{\partial y}+W\frac{\partial T}{\partial z}\right)= \Gamma.\left[\frac{\partial^2 T}{\partial x^2}+\frac{\partial^2 T}{\partial y^2}+\frac{\partial^2 T}{\partial z^2}\right] \qquad (3)$$

Boundary Conditions

Momentum Equation

Velocity and pressure boundary conditions On the wavy wall duct, the velocity fields meet no-slip wall boundary condition:

$U_{wall} = V_{wall} = W_{wall} = 0$

At the inlet of the solution domain:

Fully developed profile for velocity V with the cross velocities U = 0, W = 0

At the outlet of the solution domain:

$$\frac{\partial f}{\partial y} = 0 \quad . \quad f = \text{U, V, W, P}$$

Energy equations

Temperature field meets thermal boundary condition at the inlet:

$T = T_{in} = 40\ ^0C$

Temperature field meets thermal boundary condition at the outlet:

$$\frac{\partial T}{\partial y} = 0$$

At the wall, the thermal boundary condition:

$T = T_w = 20\ ^0C$

Numerical Model

In this study, the governing conservation equations in integral form were discretized using finite volume method [11]. The final discretized forms of governing equations are solved iteratively using TDMA solver. Iteration is continued until difference between two

consecutive field values of variables is less than or equal to 10^{-6}. For further stabilization of numerical algorithm, under relaxation factor with range from 0.4 to 0.7 for u, v, w, T, and P are used. The calculations used non-orthogonal curvilinear body fitted grid containing three dimensions 31*60*31 internal cells. The procedure used the power low scheme and simple algorithm method for pressure and velocity correction developed by Patankar [12].

The numerical solutions used elliptic grid generation technique (Poison's equation type) so as to transform geometry from curvilinear grid in physical domain in term (x, y, z) to rectangular grid in computational domain in term (x,h,z) followed the work of **Thompson,.1999 et.al [13].** Computations were performed for wavy duct with Reynolds number (100, 200 and 300), length ratio (L/2a=10, 6.67, 5) and aspect ratio (L/H = 4) and for the diverged-converged duct used Reynolds number (50, 100, 300) with height ratio (H_{min}/H_{max} = 0.46, 0.39, 0.33) and aspect ratio (L/H_{min} = 4).

The local Nusselt number on the wavy walls of the duct is defined by: :

$$Nu_{loc} = -\frac{\frac{\partial T}{\partial x}.D_h}{(T_w - T_{in})} \quad \text{…..…..…….. (4)}$$

$$\frac{\partial T}{\partial x} = \left[\left(\frac{\partial T}{\partial x}\right)^2 + \left(\frac{\partial T}{\partial z}\right)^2\right]^{1/2} \quad \text{…..…… (5)}$$

The average Nusselt number is defined by the following relation:

$$Nu_{avg} = \frac{1}{N}\sum_{j=2}^{j=Nj-1} Nu_{loc} \quad \text{…..…… (6)}$$

While the Reynolds number is defined as:

$$\mathrm{Re} = \frac{D_h r v_{avg}}{m} \quad \text{…… (7)}$$

where D_h is the hydraulic diameter.
While the shear stress is defined as:

$$t_w = m\frac{U_p}{x_p} \quad \text{……. (8)}$$

where

$$U_p = \sqrt{U^2 + V^2 + W^2}$$

and

x_p is the normal distance between the near-wall grid mode (p) and the wall.

Model Validation

The model validation is an essential part of a numerical investigation. Validation of the present study has been performed for the laminar flows in a diverged-converged duct and compared with pervious work for Bahaidarah et.al [9]. The comparison was conducted for (Re = 25 and 100) and Pr = 0.7. Good agreement was achieved as illustrated in fig (2) and fig (3) that show the results of this work together with the numerical results of Bahaidarah et.al [9] in streamlines and temperature contours respectively. Table (1) shows the comparison of average Nusselt number on the wavy wall with the numerical results of Bahaidarah et.al [9].

Result and Discussion

Flow field and temperature

Streamlines and velocity vector for flows with Re=100, 200,300 and length ratio (L/2a=10, 6.67 and 5) are shown in figures (4, 5, 6) respectively for wavy duct. Lateral vortex is trigged at the Re=300 and (L/2a=6.67). With increasing flow rate and length ratio led to increase in the lateral swirl. At a very low Reynolds number, however, viscous forces dominate to produce undisturbed streamline flows and vortex is not developed, irrespective of the length ratio. The temperature contour distribution in water (Pr=5.85) flows shown in figures (4, 5, 6). The increasing special coverage of the trough vortices with Re and length ratio results more uniform core region temperature

distributions and the overall convection heat transfer increases.

Streamlines and velocity vector for flows with Re=100,200,300 and height ratio (H_{min}/H_{max}=0.46, 0.39, 0.33) are shown in figures (7, 8, 9) for diverged-converged duct. Lateral swirl is trigged at the Re=100 and (H_{min}/H_{max}=0.46). With increasing Reynolds number and decreasing height ratio led to increase lateral vortex. The temperature couture distribution at Pr = 0.7 shown in figures (7, 8, 9), the increase of flow rate and decrease of height ratio results more core region temperature distribution and increasing of overall heat transfer.

Local Nusselt Number

For wavy duct, Fig (10) shows the variation of Nusselt number with axial direction for Pr = 0.7, while fig (11) shows the same relation but for Pr = 5.85. It is obvious from fig (10) that the maximum Nusselt number takes place at the inlet for length ratio equal 10. A decrease in the length ratio causes a decrease in Nusselt number at the inlet. The maximum value of the Nusselt number decreases with decreasing the length ratio. It is clear from fig (10) that the location of the minimum local Nusselt number remains almost at the same place. It is clear from fig (11), that the maximum local Nusselt number takes place at about 25% from the inlet location for all length ratios. A decrease in the length ratio causes an increase in the maximum Nusselt number. Regarding the minimum local Nusselt number for Pr = 5.85, fig (11) shows a slight decrease with decreasing length ratio.

For diverged-converged duct, Fig (12) shows the variation of Nusselt number with axial direction for Pr = 0.7, while Fig (13) shows the same relation but for Pr = 5.85. It is obvious from figure (12) that the local Nusselt number decreases rapidly with axial direction and becomes minimum approximately at the center of the duct. Thereafter, it increases slightly with axial direction for any height ratio. A decrease in the height ratio causes a slight shift of the curves downward. Figure (13) shows that the lowest Nusselt number takes place when the Reynolds number approaches 50. An increase in Reynolds number to 300 leads that to increase in the value of the minimum local Nusselt number. This phenomenon occurs for all height ratios. However, a decrease in the height ratio causes the curves to be closer to each other especially for height ratio equal 0.33. Also for a given Reynolds number, the minimum value of the local Nusselt number increases with decreasing of the height ratio.

Shear Stress

For wavy duct, figure (14) and (15) show the variation of the shear stress with axial direction for a Prandtl number of 0.7 and 5.85 respectively. It is clear from these figures, that the effect of decrease in length ratio is quite pronounced at the location of swirl near the axial direction at 70% from the inlet location. At this location, the shear stress increases with increasing Reynolds number for any length ratio. However, the decrease in length ratio causes a significant increase in shear stress. It is worthwhile mentioning that the shear stress peak in fig (15) for Pr=5.85 in about twice that for Pr=0.7 shown in fig (14).

Figures (16) and (17) show the variation of shear stress with axial direction for a Prandtl number of 0.7 and 5.85 respectively for diverged-converged duct. It is obvious from fig (16) that the behavior of shear stress versus axial direction for Prandtl number of 0.7 is quite similar to that of fig (17) for Pr=5.85. It is obvious from fig (16) that for a given height ratio, an increase in Reynolds number causes the curves to be shifted upward. It is interesting to note that for a Reynolds number of 300, a decrease in height ratio causes the curve for shear stress to have a small peak at the axial direction at end of the swirl. However, the magnitude of shear stress for Pr=0 .7 is about half that for Pr=5.85.

Average Nusselt Number

Figure (18) for wavy duct with Pr=0.7 shows that the average Nusselt number increases with Reynolds number.

However, when the ratio (L/2a) decreases from infinity to (10) causes the curve to be shifted upward resulting into an increase in the average Nusselt number. A further decrease in (L/2a) ratio from 6.67 to 5 causes a decrease in the average Nusselt number. Figure (19) for wavy duct with Pr=5.85 is similar to figure (18) but the rate of increase of the average Nusselt number with Reynolds number is much lower than that for figure (18). However, the average Nusselt number in fig (19) for the same (L/2a) ratio is much higher than that of figure (18).

Figure (20) for diverged-converged duct with Pr=0.7 and height ratio (H_{min}/H_{max}) equal 0.46, the average Nusselt number increases with increasing Reynolds number. A decrease of (H_{min}/H_{max}) ratio leads to a decrease in average Nusselt number. The average Nusselt number at (H_{min}/H_{max}=1) becomes maximum. Figure (21) for diverged-converged duct with Pr=5.85 and height ratio (H_{min}/H_{max}) equal 0.46, the average Nusselt number increases with increasing Reynolds number. A decrease in (H_{min}/H_{max}) ratio leads to a decrease in the average Nusselt number. The average Nusselt number becomes minimum at (H_{min}/H_{max}=1).

Conclusion

1. For air heat exchanger it can be concluded that the wavy duct perform better than the diverged-converged duct in term of average Nusselt number.
2. The water heat exchanger performance was found to be approximately similar for wavy and diverged-converged ducts.
3. The local Nusselt number, average Nusselt number and shear stress increase with increasing of Reynolds number.
4. the maximum average Nusselt number for diverged-converged ducts took place at a height ratio (H_{min}/H_{max}=1) at Pr=0.7, while the maximum took place at height ratio (H_{min}/H_{max}=0.46) for Pr=5.85.
5. For wavy duct at Pr=0.7 and Pr=5.85 the maximum average Nusselt number takes place at length ratio (L/2a=10).
6. For diverged-converged and wavy duct at Pr=0.7 and 5.85, the shear stress increases with increasing height and length ratio.
7. It is clear from study that the transfer by diffusion are more significant in water (Pr=5.85) than in air (Pr=0.7).
8. There is good agreement between the results of this work with the corresponding numerical results presented by Bahaidarah [9]

Reference

[1] S.D.Hwang, I.H.Jang and H.H.cho, **"Experimantal study on flow and local heat/mass transfer characteristics inside corrugated duct"**, International Journal of heat and fluid flow 27(2006)21-32.

[2] T.Adachi and H.Uehara, "**pessure drop and heat transfer in spainwise periodic fluted channels**:, Numercal heat transfer, part A, 43;47-64,2002

[3] H.Blomerius and N.K.Mitra, "**Numerical investigation of convective Heat transfer and pressure drop in wavy duct**", Numerical Heat transfer, Part aA, 37;37-54, 2000

[4] K.stone and S.P.Vanka, **"Numerical study of Developing Flow and heat transfer in a wavy passage",** Journal of fluid Engineering, December 1999, Vol.121.

[5] M.Molla, A.Hossain and L.yao, **"Natural-convection flow along a vertical complex wavy surface with uniform heat flux"**, Journal of heat transfer, October 2007, Vol.129.

[6] N.Mouhamad, B.Khedidja and Z.Belkacem, **"Numerical Analysis of flow and heat transfer in the entrance region of a wavy channel with thermal Asymmetric walls"**, International Journal of applied Engineering, research IssNo973-4562 Volume 1 Number 2(2006) pp.273-293.

[7] Raj M.Manglik, Jiehai Zhang, Arun Muleg**, " Low Reynolds number forced convection in three-dimensional wavy-plate-fin compact channels fin density effects",** International Journal of heat transfer 48(2005) 1439-1449.

[8] M.Z.Hossain and A.K.M.Sadrul Islam, **"Numeral investigation of fluid flow and heat transfer characteristics in sine, triangular, and Arc-shaped channels",** Thermal science: Vol, 11(2007), No.1, pp.17-26.

[9] Haitham M.S.Bahaidarah, N.K.Anand, and H.C.Chen, **"Numerical study of heat and momentum transfer in channels with wavy walls"**, Numerical Heat Transfer, part A, 47:417-439,2005.

[10] M.Gradeck, B.Hoaread and M.Lebouche **"Local analysis of heat transfer inside corrugated channel"**, International Journal of heat and mass transfer 48(2005)1909-1915.

[11] Versteeg H.K., Masasekera W., **"An introduction to computational fluid mechanics"** , Longman Group Ltd, 1995.

[12] Patankar S.V., **"Numerical Heat transfer and fluid Flow"**, Hemisphere Puplishing Corporation, 1980.

[13] Joe F. Thompson, bharat K. soni and Nigel P weatherill, **"Grid generation",** New York, Washington, London, 1999.

Table (1) shows the comparison of average Nusselt number on the wavy wall with the numerical results of Bahaidarah et.al [9] at H_{min}/H_{max}=0.3 and L/2a=4.

Reference	Re=25	Re=100	Re=400
Bahaidarah	8.7739	9.1764	11.5474
Present work	7.72	8.21	9.98

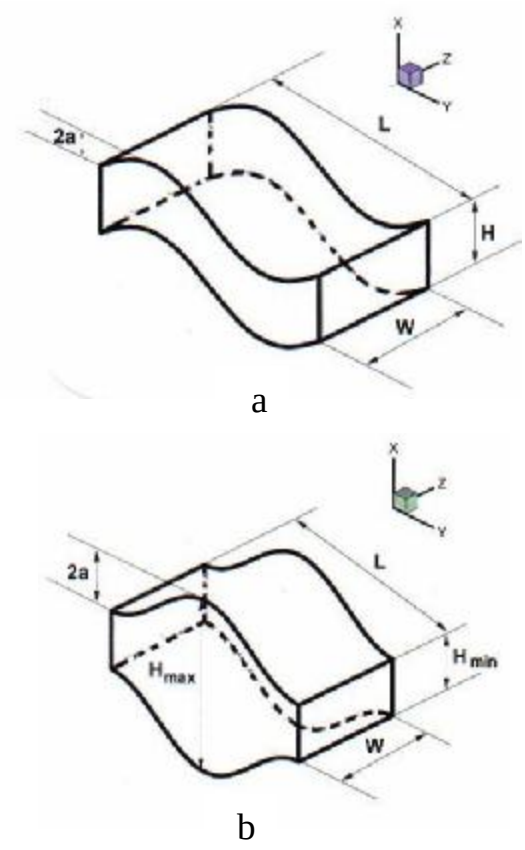

Figure (1) Geometric configurations of a: wavy duct, b: diverged-converged duct

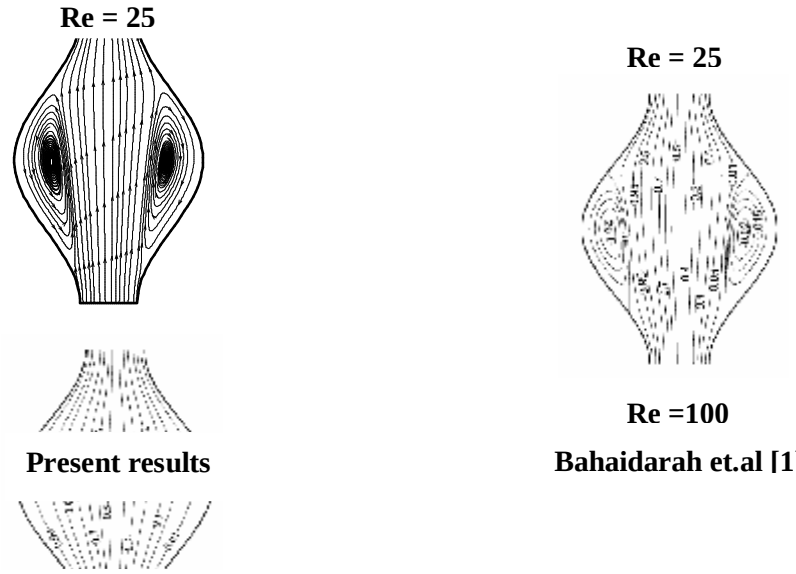

Figure (2) Comparison of the streamlines between the present work and that of Bahaidarah et.al [9] using Re = 25 and Re = 100, H_{min}/H_{max}=0.3 and L/2a=4

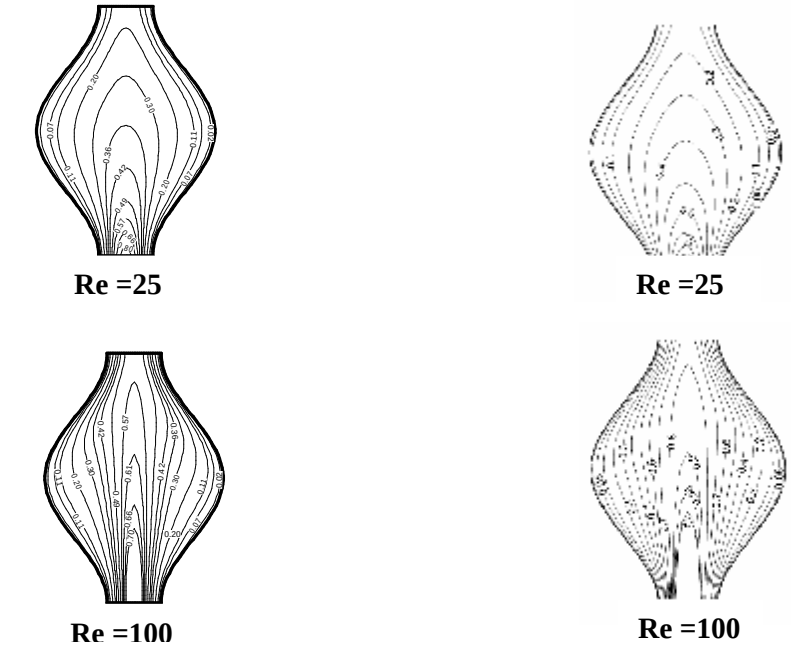

Figure (3) Comparison of the temperature contours between the present work and that of Bahaidarah et.al [9] using Re = 25 and Re = 100, H_{min}/H_{max}=0.3 and

Relative (Cm/Magnitude) = 35

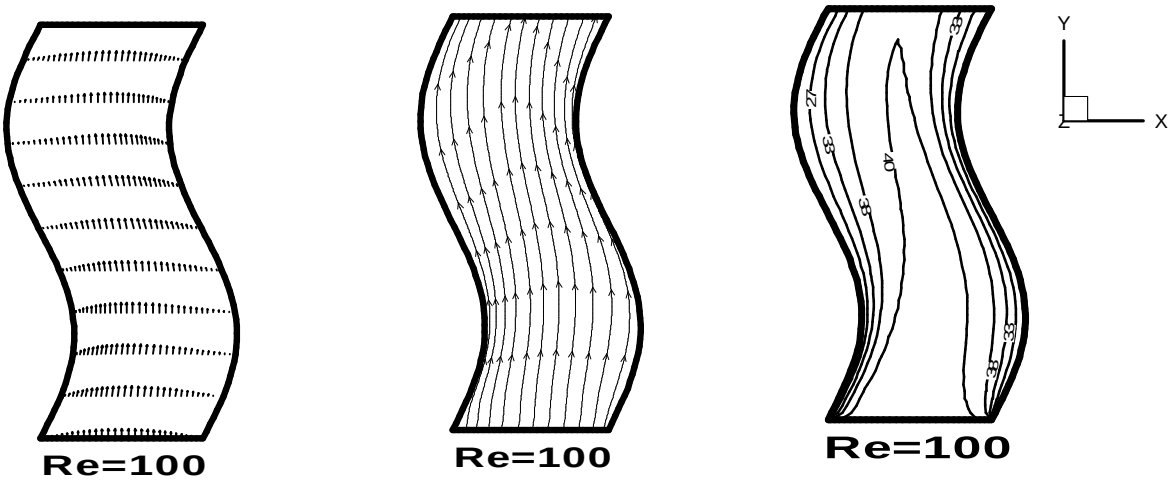

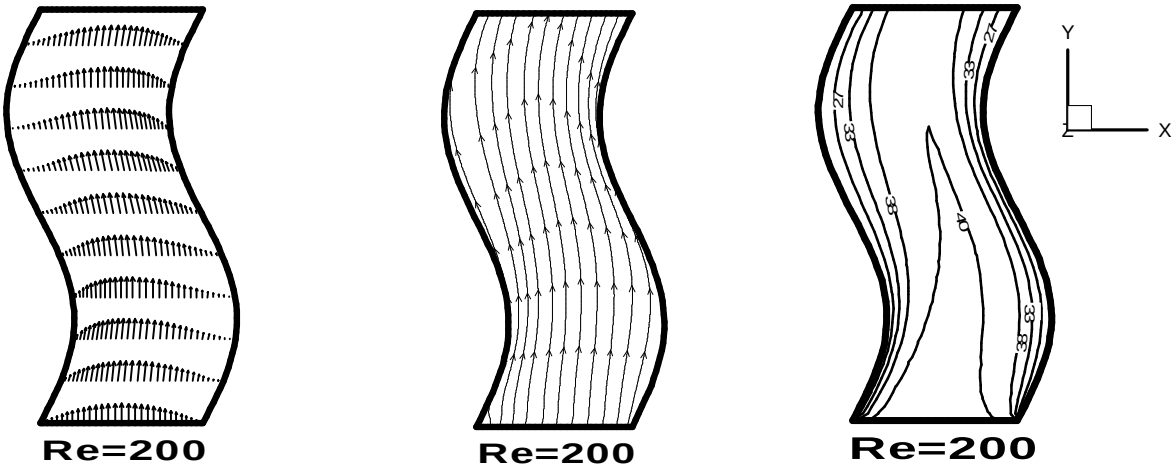

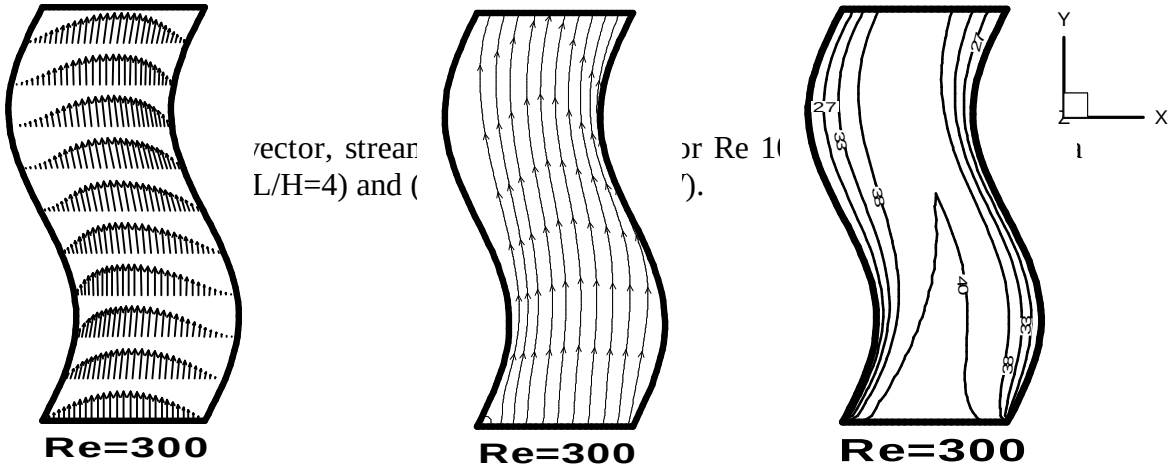

F ...ector, strean... ...or Re 1... ...
P ... L/H=4) and (...).

Relative (Cm/Magnitude) = 35

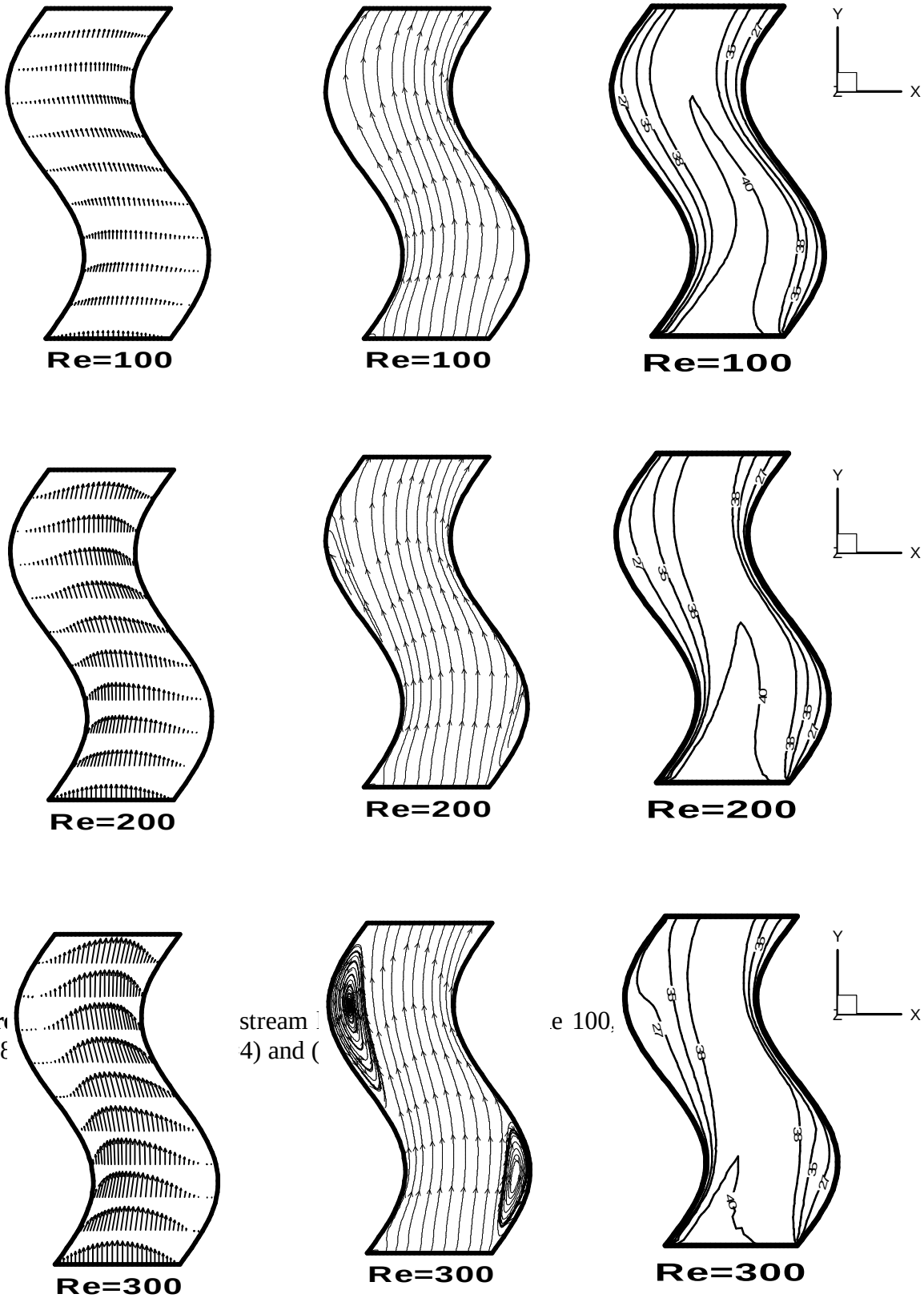

Figur stream e 100, Pr=5.8 4) and (

Relative (Cm/Magnitude) = 35

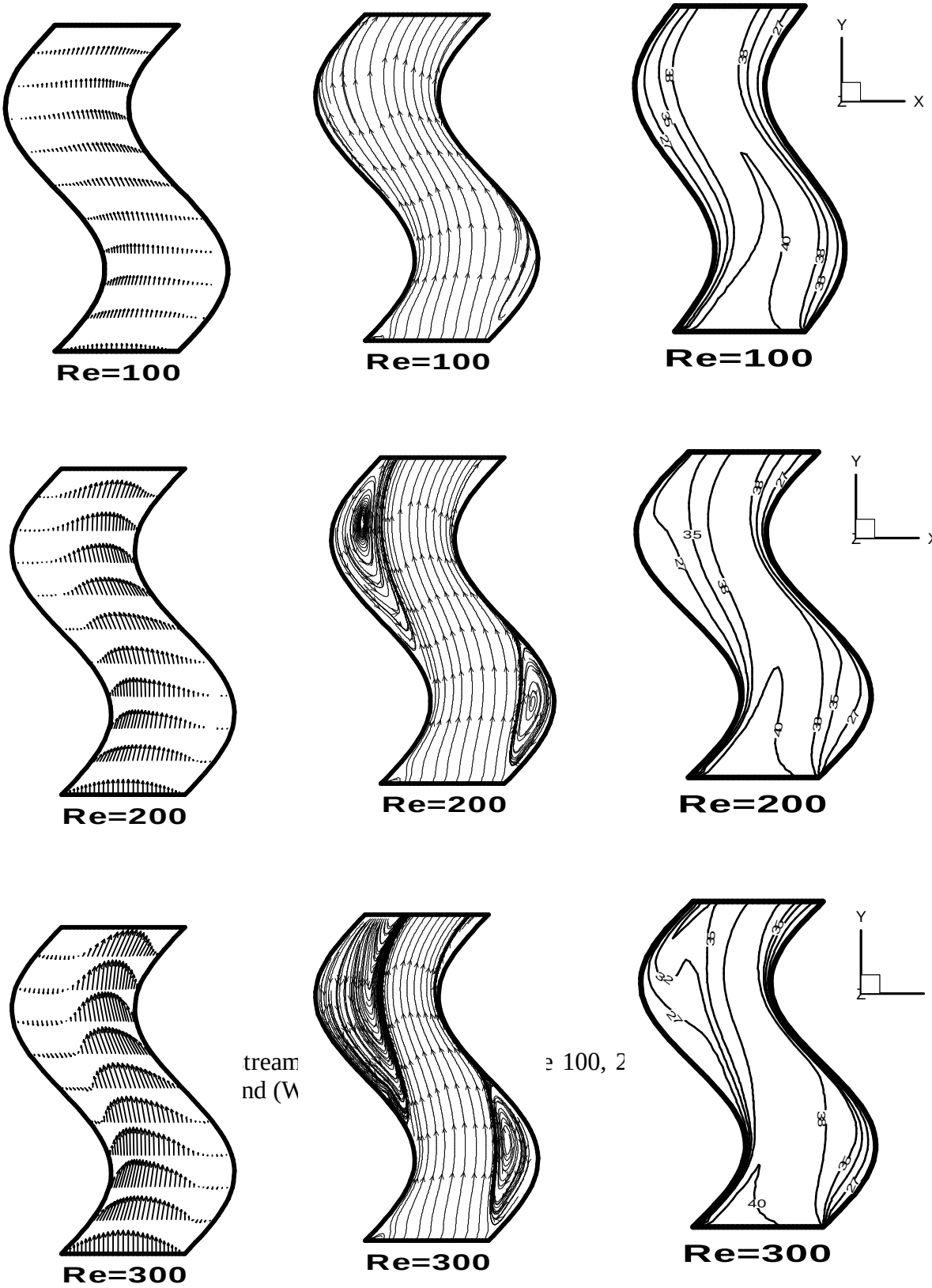

Figu tream e 100, 2
Pr=5. nd (W

Relative (Cm/Magnitude) = 3.5

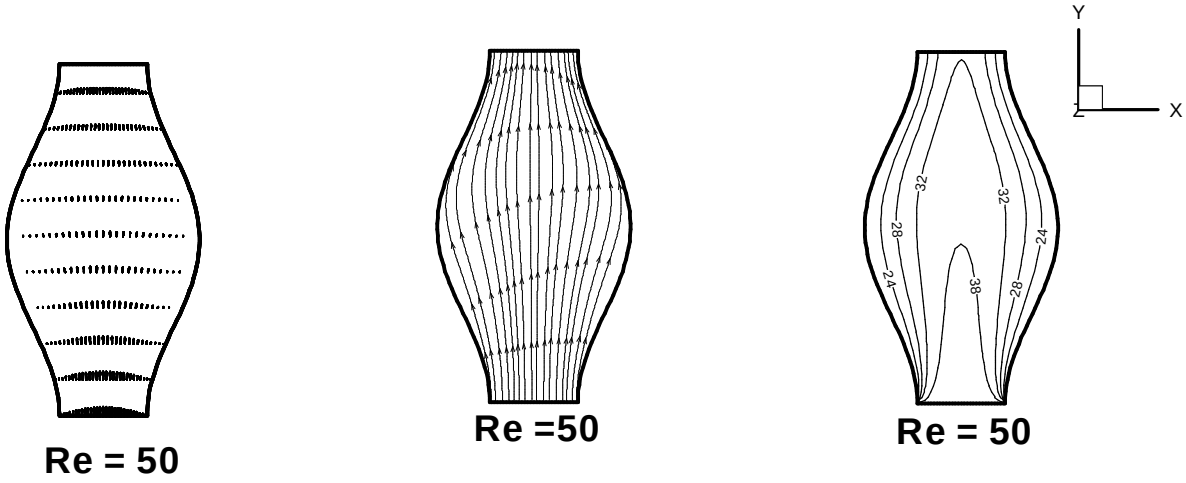

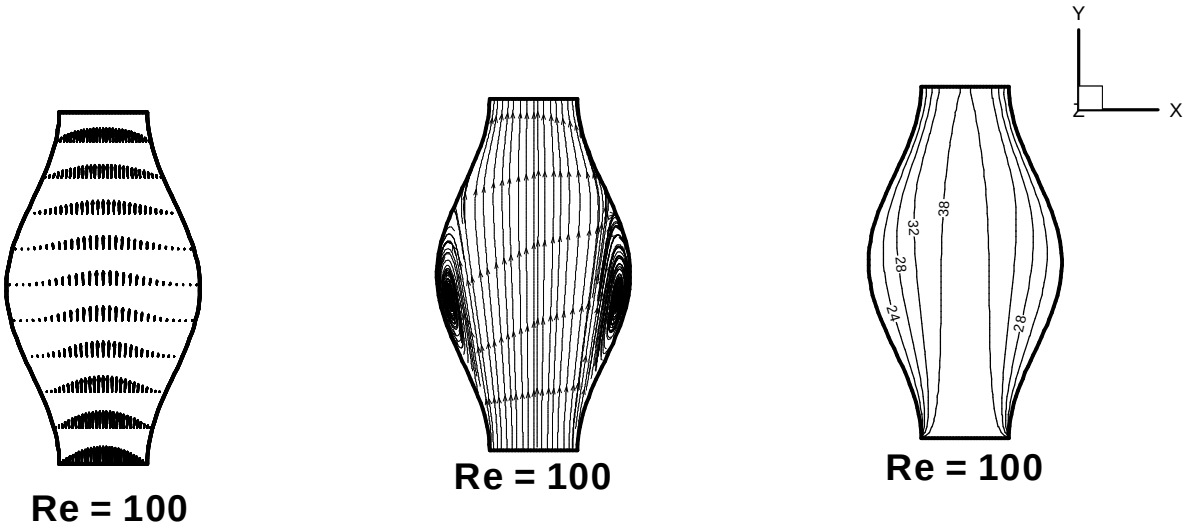

Figure (7) Velocity vector, stream l for Re 100, 200
P x=0.46), (L/Hmi) at (Z=0.5W).

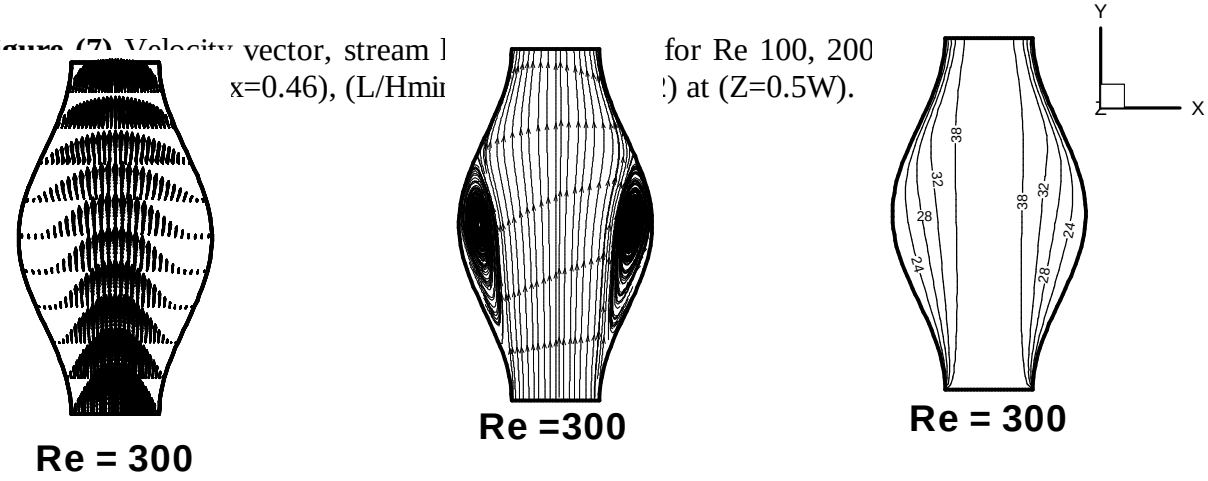

Relative (Cm/Magnitude) = 3.5

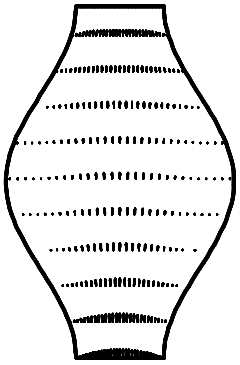

Re = 50

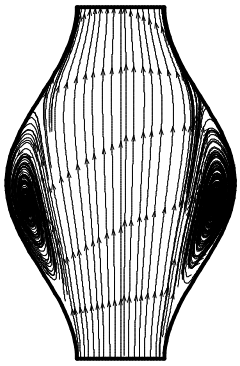

Re =50

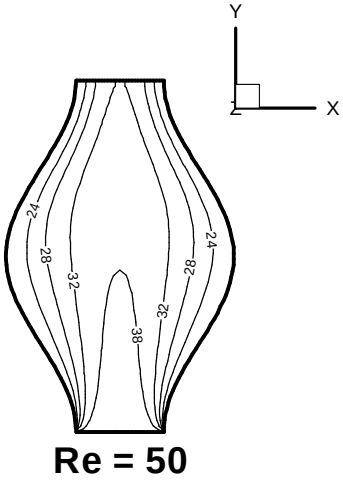

Re = 50

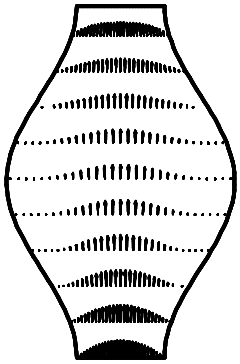

Re = 100

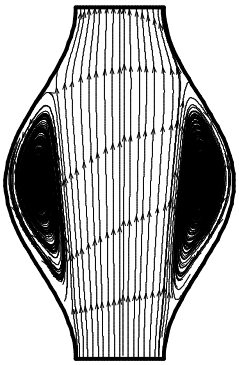

Re =100

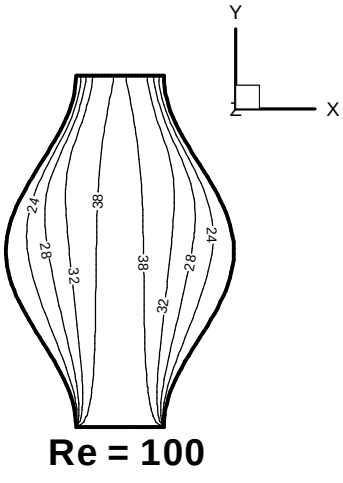

Re = 100

Fi ector, strea r Re 100, Z
Pr =0.39), (L/H at (Z=0.5W

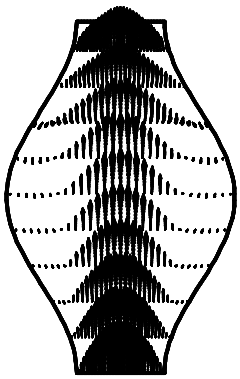

Re = 300

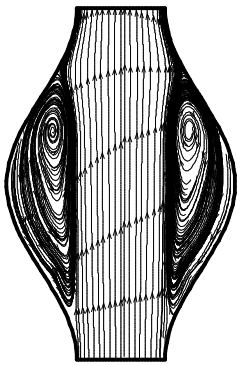

Re =300

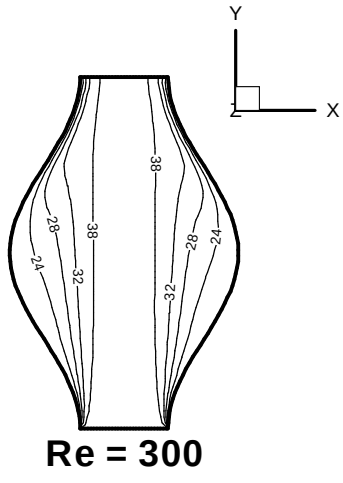

Re = 300

Relative (Cm/Magnitude) = 3.5

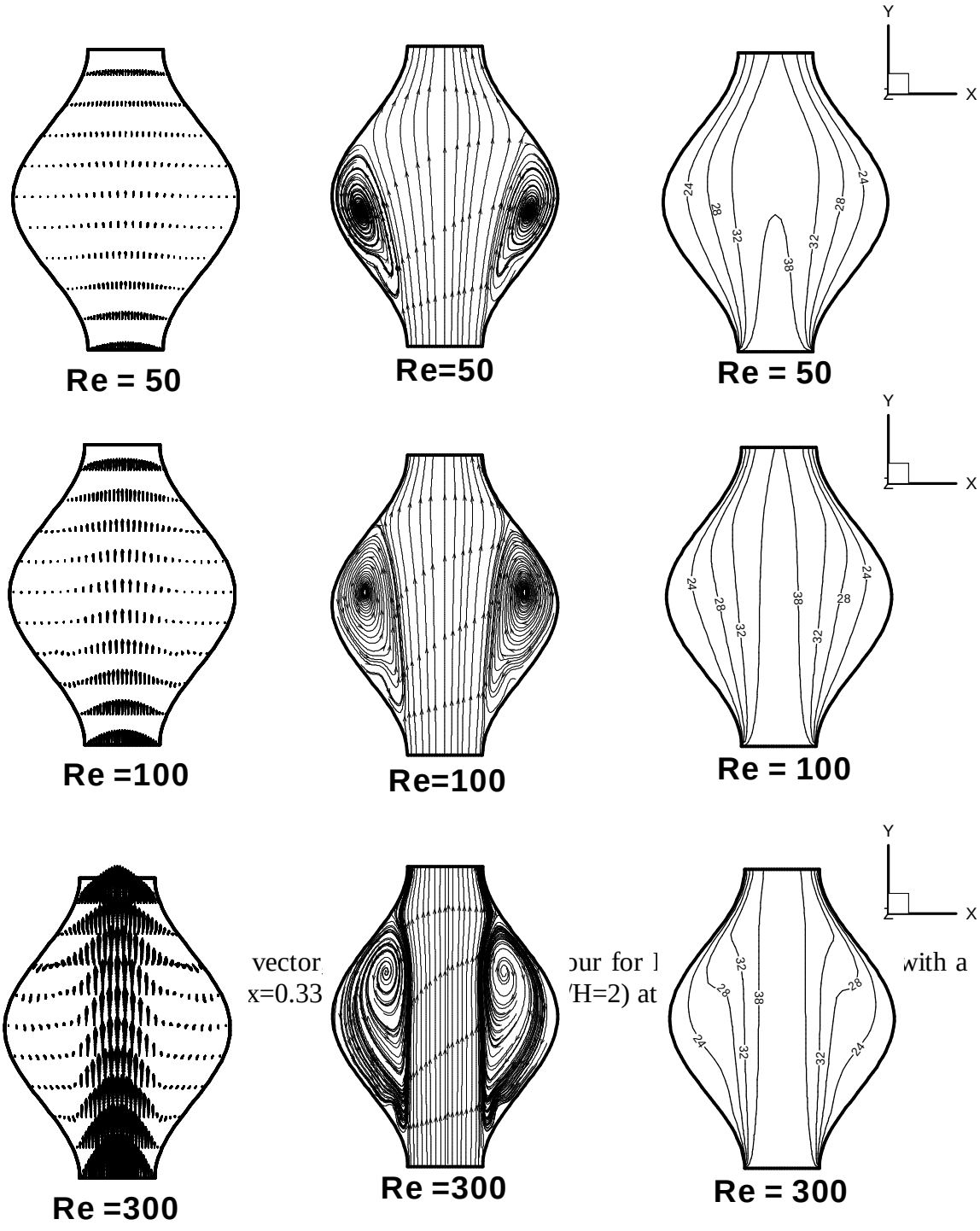

vector ...our for l ...with a x=0.33 ...H=2) at

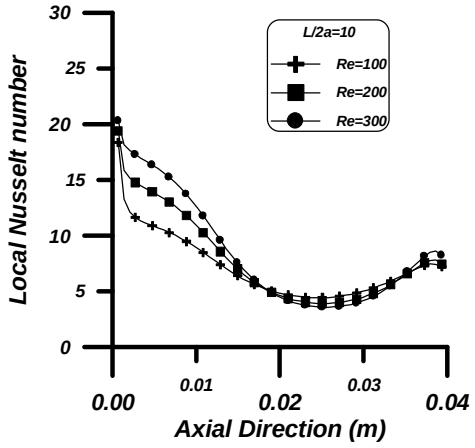

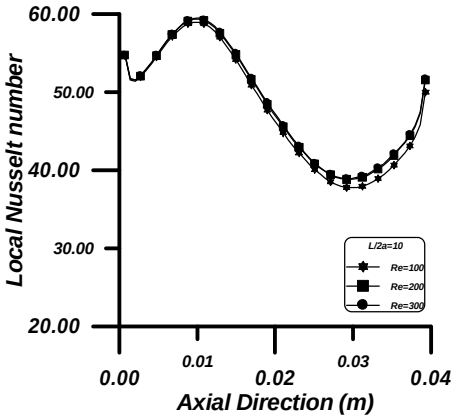

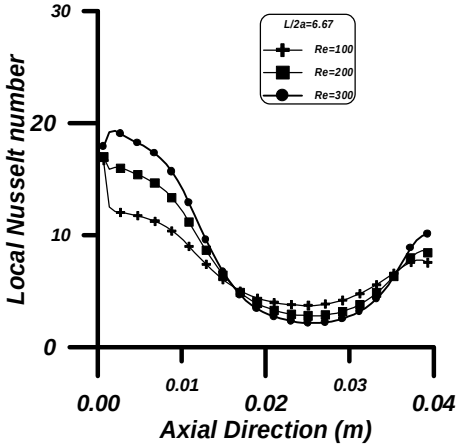

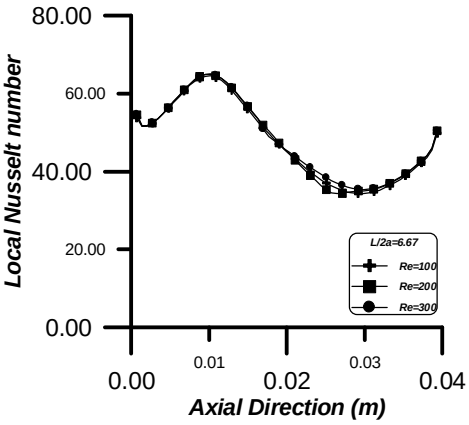

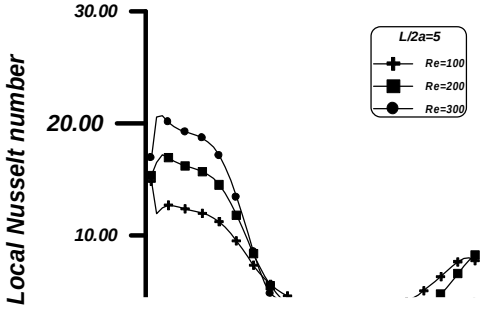

Figure (10) Local Nusselt number distribution in wavy duct at Pr = 0.7 and length ratio equal 10, 6.67 and 5.

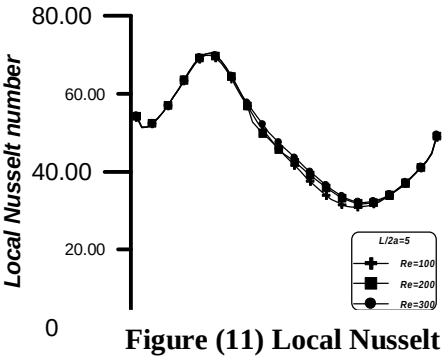

Figure (11) Local Nusselt number distribution in wavy duct at Pr = 5.85 and length ratio equal 10, 6.67 and 5.

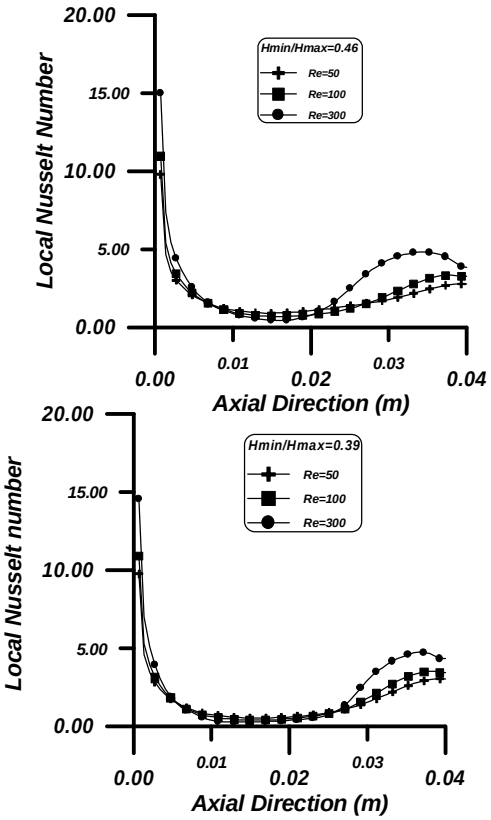

Figure (12) Local Nusselt number distribution in diverged-converged duct at Pr = 0.7 and height ratio equal 0.46, 0.39 and 0.33.

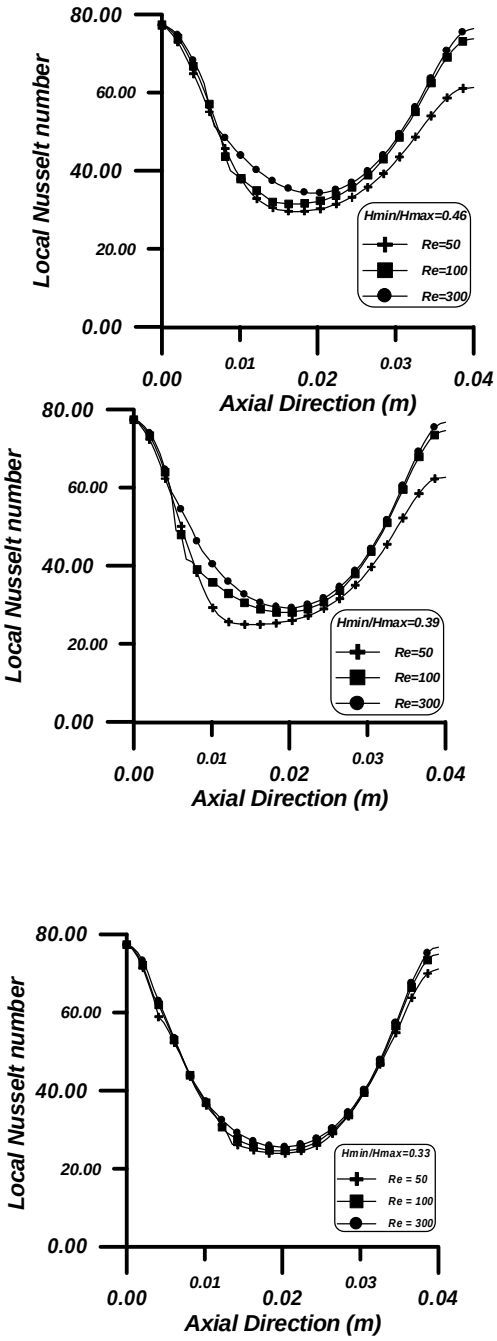

Figure 13: Local Nusselt number distribution in diverged-converged duct at Pr = 5.85 and height ratio equal 0.46, 0.39 and 0.33.

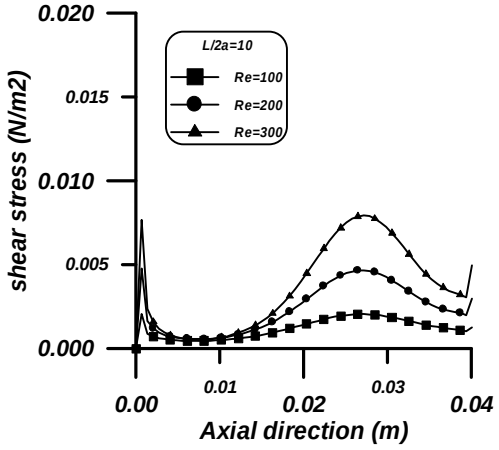

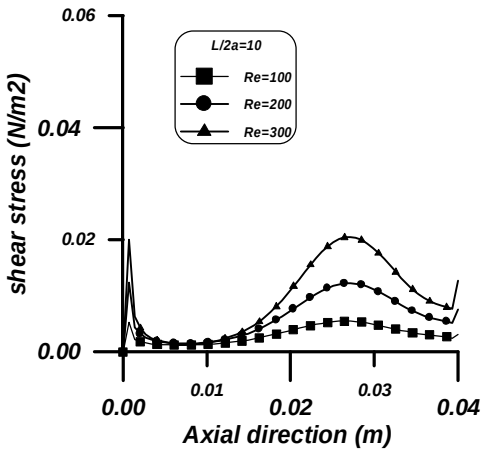

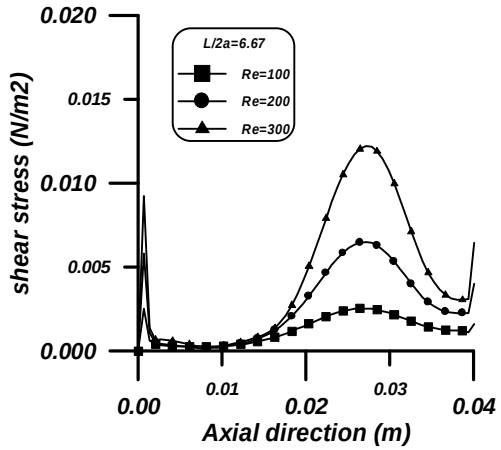

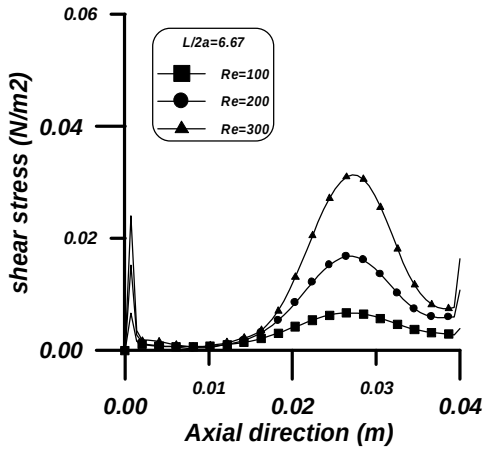

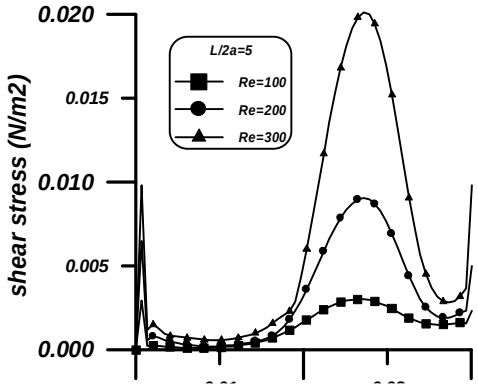

Figure (14) Shear stress versus axial direction for wavy duct at Pr=0.7

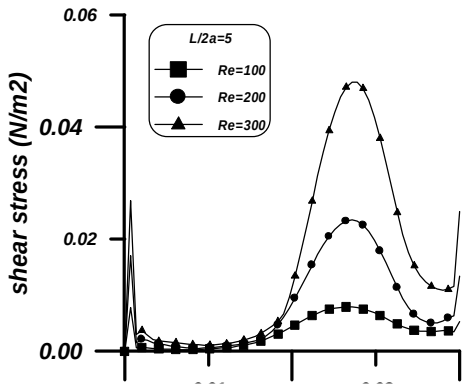

Figure (15) Shear stress versus axial direction for wavy duct at Pr=5.85

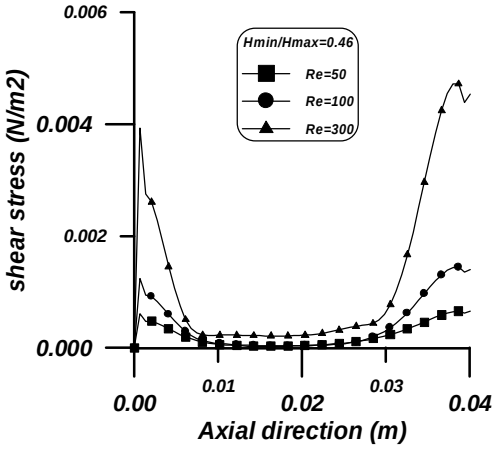

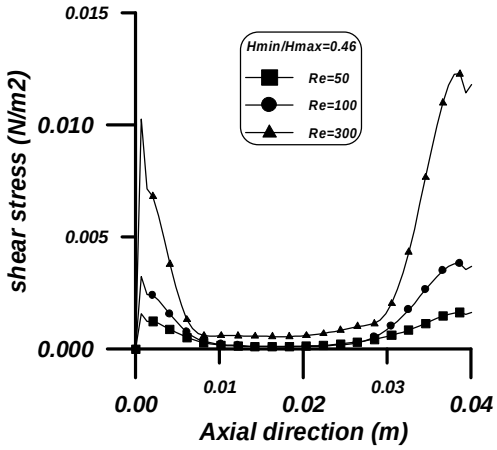

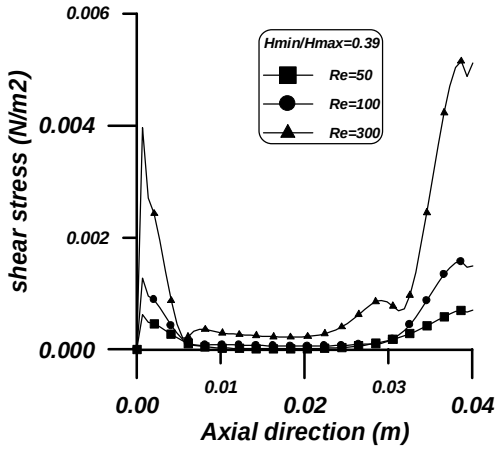

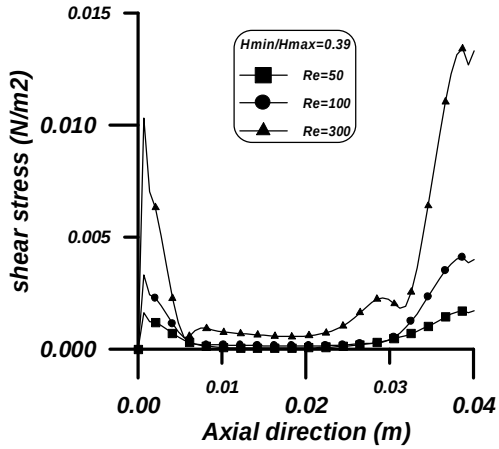

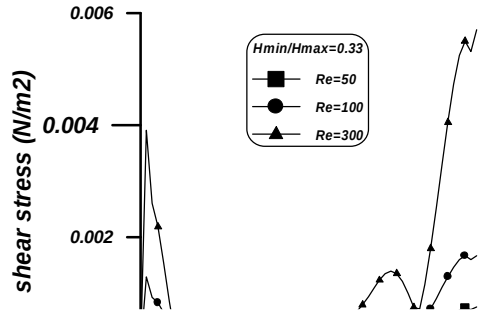

0 **Figure (16) Shear stress versus axial direction for diverged-converged duct at Pr=0.7**

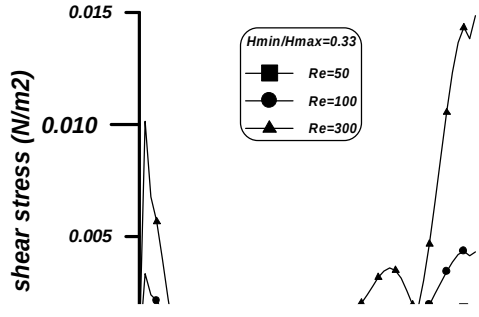

0.(**Figure (17) Shear stress versus axial direction for diverged-converged duct at Pr=5.85**

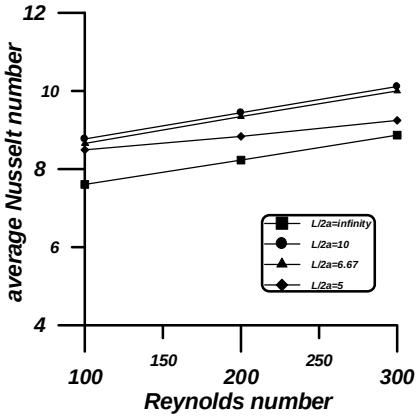

Figure (18) Distributions of the average Nusselt number for wavy duct at Pr = 0.7

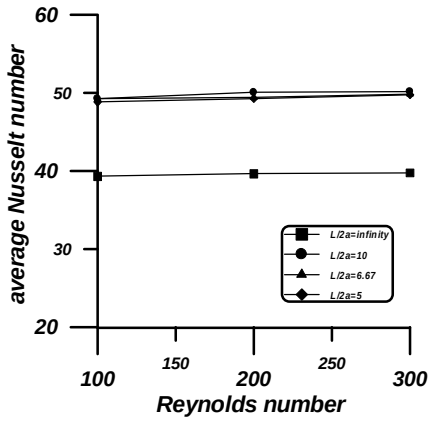

Figure (19) Distributions of the average Nusselt number for wavy duct at Pr = 5.85

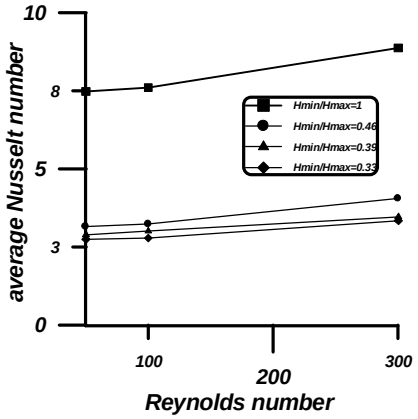

Figure 20: Distributions of the average Nusselt number for diverged-converged duct at Pr =

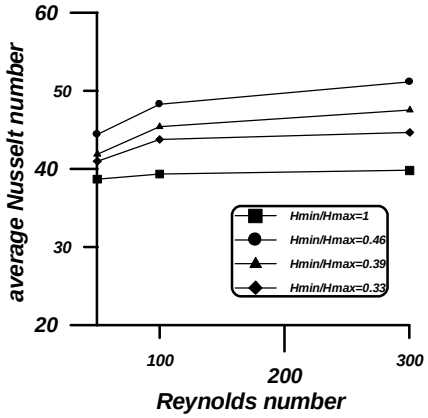

Figure 21: Distributions of the average Nusselt number for diverged-converged duct at Pr = 5.85